This is the Pre-Published Version.

This version of the article has been accepted for publication, after peer review (when applicable) and is subject to Springer Nature's AM terms of use (https://www.springernature.com/gp/open-research/policies/accepted-manuscript-terms), but is not the Version of Record and does not reflect post-acceptance improvements, or any corrections. The Version of Record is available online at: http://dx.doi.org/10.1007/s11440-022-01741-z.

Finite element model and simple method for predicting consolidation displacement of soft soils exhibiting creep underneath embankments in 2-D condition

Ze-Jian Chen (Postdoctoral Fellow)
Department of Civil Engineering, The Hong Kong Polytechnic University, Hong Kong SAR, China
Email: ze-jian.chen@connect.polyu.hk
ORCID: https://orcid.org/ 0000-0001-7855-6234

Wei-Qiang Feng (Assistant Professor, Corresponding Author)
Department of Ocean Science and Engineering, Southern University of Science and Technology, Shenzhen, China
Email: fengwq@sustech.edu.cn
ORCID: https://orcid.org/0000-0001-5480-9719

and
Jian-Hua Yin (Chair Professor)
Department of Civil Engineering, The Hong Kong Polytechnic University, Hong Kong SAR, China
Research Institute of Land and Space, The Hong Kong Polytechnic University, Hong Kong SAR, China
Email: cejhyin@polyu.edu.hk
ORCID: https://orcid.org/0000-0002-7200-3695

Revised manuscript submitted to *Acta Geotechnica* for possible publication as a research article

Abstract: How to predict the long-term deformation of natural soft soils under embankments has been an important yet challenging issue in geotechnical and transportation engineering. The major difficulties lie in consolidation analyses of thick soil layers, modelling of the nonlinear time-dependent stress-strain behaviour of clayey soils, and proper determination of soil parameters. While finite element (FE) software has great advantages and wide applications in consolidation analyses, development of reliable simple methods, which can be conveniently used by engineers, is also needed. In this paper, both a fully coupled FE model and a simplified Hypothesis B method are developed and applied for long-term deformation analyses of two test embankments on the multi-layered Malaysian marine clays. FE simulations are conducted using PLAXIS with a nonlinear 3-D elastic visco-plastic (3-D EVP) model. A series of parametric studies are carried out on the influences of soil parameters and modelling techniques using this FE model. A simplified Hypothesis B method with the nonlinear 1-D EVP model and modifications for 2-D stress diffusion and buoyancy effects is derived and applied for estimating the long-term consolidation settlement curves of the two test embankments. It is found that the fully coupled FE model with the nonlinear 3-D EVP can simulate the long-term embankment displacements with good agreement with measured data. Parametric studies indicate that using averaged soil indices and updating static pore pressure have significant contributions to the accuracy of simulations. The settlements calculated by the improved simplified Hypothesis B method are found in close agreement with FE simulation results and measured data.

Keywords: soft soils, embankments, consolidation settlement, elastic visco-plastic model, buoyancy

1 Introduction

In recent decades, large numbers of infrastructure facilities such as airports, artificial islands, highways, railways and ports are under planning, construction or service in coastal regions of many countries. There exists a heavy demand for embankment constructions on soft marine soils. Many engineering problems and difficulties related to soft soils have been recognized and reported, such as excessive and continuous settlements, embankment failure, and low speed of consolidation (Folkes and Crooks 1985; Loganathan et al. 1993; Fatahi et al. 2013). Reliable evaluation and prediction of the long-term behaviour of soft soils under human activities and external loadings are still challenging issues.

There are two major factors contributing to the time-dependent deformation of soft soils: the consolidation due to gradual dissipation of excess pore water pressure and the creep behaviour of soil skeleton. Analysis of 1-D consolidation is usually based on Terzaghi's 1-D consolidation theory (Terzaghi 1943), and its extended analytical solutions for complicated consolidation problems subjected to multi-layered system, vertical drains, and ramp loadings (Hansbo et al. 1981; Zhu and Yin 2004; Walker et al. 2009; Yin and Zhu 2020). For 3-D consolidation analysis, Biot's 3-D consolidation equations (Biot 1956) are most frequently used. The creep behaviour is usually defined as continuous and time-dependent compression of soils under constant effective stress, which is a result of the viscous nature of clayey soils (Feng et al. 2017; Shi et al. 2018). The viscous behaviours of soils include all time-dependent stress-strain behaviours, such as creep, strain rate effect and relaxation. To simulate these effects, researchers have developed 3-D constitutive elastic visco-plastic (EVP) models for clayey soils (Borja and Kavazanjian 1985; Yin and Graham 1999; Vermeer and Neher 1999; Yin et al. 2010). In these constitutive models, the creep of soils is modelled based on an empirical linear formula between the volumetric strain and logarithm of time (*i.e.* $\Delta\varepsilon = \frac{C_{\alpha e}}{1+e_0}\log t$ or $\Delta\varepsilon = \frac{\psi}{1+e_0}\ln t$) (Ladd et al. 1977; Yin and Graham 1989). Although such relations can achieve satisfactory simulations within a relatively shorter period (*e.g.* several months or years), concerns have been raised about the infinite creep with time in the formula. A nonlinear logarithmic function for creep was then proposed by Yin (1999), which contains a creep limit at infinity of time. The function was later introduced into a 3-D EVP model (Yin et al. 2002) based on the overstress theory (Perzyna 1963). In theory, this model has advantages in simulating the long-term deformation of clayey soils. However, case studies on natural soil ground are still less reported.

Considering the highly nonlinear partial differential equations in both the EVP models and consolidation theory, researchers have relied on finite difference methods (FDM) and finite element methods (FEM) to simulate the coupled effect of consolidation and rheology of soils. Despite of the tremendous advantages of FDM and FEM, the convergence and accuracy of calculations are influenced by the scheme of time steps and proper setting of the numerical models, especially for 3-D or 2-D conditions. In some recent works, de-coupled simplified methods are also being developed with 1-D creep model and conventional theoretical consolidation solutions (Yin and Feng 2017; Feng and Yin 2017, 2018; Feng et al. 2020). However, these simplified methods are still limited to 1-D consolidation condition and their applicability in some embankment analyses is questioned. The nonlinear creep behaviour and the buoyancy effects have not been considered in these studies as well. Besides, the accuracy of FEM, FDM and simplified method relies on parameter selections, which is greatly influenced by the soil uncertainty and experimental technology.

To address these issues, this paper will present the methodologies of both FE method and simple method using a nonlinear EVP model with consideration of creep limit for the Malaysian test embankments, which will be examined by measured data. Parametric studies are carried out to reveal the optimization scheme of soils parameter and controlling parameters in the fully coupled FE analysis. A new simplified method based on Hypothesis B with modifications for 2-D stress diffusion and buoyancy effects is proposed and examined by comparison with FE simulation results and measured data. The results show clear evidence for both the accuracy and practicality of the EVP model in predicting the long-term consolidation deformation of soft soil ground under embankments with complicated field conditions.

2 Theoretical frameworks of the 1-D and 3-D nonlinear EVP model

2.1 1-D nonlinear creep model for clayey soils

It is widely acknowledged that the stress-strain behaviour of clayey soils is time-dependent (Graham et al. 1983; Leroueil et al. 1985; Yin and Graham 1989). One popular way to model the time dependency of soil behaviour is based on the simulation of creep behaviour with mathematical equations. Creep refers to the time-dependent deformation of soil under constant effective stress. In odometer tests, if a normally consolidated clay is subjected to a constant vertical effective stress and sustained for a period, the creep deformation can be described using Yin (1999)'s nonlinear equation:

$$\varepsilon_{creep} = \frac{\frac{\psi_0}{V}\ln\left(\frac{t+t_0}{t_0}\right)}{1+\frac{\psi_0}{V\Delta\varepsilon_l}\ln\left(\frac{t+t_0}{t_0}\right)} \quad (1)$$

where ψ_0 is the creep coefficient, $V=1+e_0$ is the initial specific volume, t is time, $\Delta\varepsilon_l$ is the creep limit and t_0 is a reference time (*e.g.* one day in standard oedometer tests). According to this function, there is an upper limit of creep deformation, as shown in Eq. (2):

$$\lim_{t\to\infty} \varepsilon_{creep} = \Delta\varepsilon_l \tag{2}$$

Fig.1 shows the schematic diagram of the 1-D EVP model for this study. The reference time line corresponds to the normal compression line measured at t_0 in conventional multi-staged oedometer tests. Based on Eq.(1) and the concept of equivalent time by Yin and Graham (1989, 1994), the 1-D strain of clay is expressed in the following equation:

$$\begin{aligned}\varepsilon_z &= \varepsilon_{z0} + \frac{\kappa}{V}\ln\frac{\sigma'_{zp}}{\sigma'_{z0}} + \frac{\lambda}{V}\ln\frac{\sigma'_z}{\sigma'_{zp}} + \frac{\frac{\psi_0}{V}\ln\left(\frac{t_e+t_0}{t_0}\right)}{1+\frac{\psi_0}{V\Delta\varepsilon_l}\ln\left(\frac{t_e+t_0}{t_0}\right)} \\ &= \varepsilon_z^r + \frac{\frac{\psi_0}{V}\ln\left(\frac{t_e+t_0}{t_0}\right)}{1+\frac{\psi_0}{V\Delta\varepsilon_l}\ln\left(\frac{t_e+t_0}{t_0}\right)}\end{aligned} \tag{3}$$

where σ'_z, ε_z is the current effective stress and strain, $V = 1+e_0$ is the initial specific volume, κ is the slope of instant time line (unloading/re-loading line) on the $e-\ln p'$ curve, λ is the slope of reference time line (normal compression line) on the $e-\ln p'$ curve, σ'_{zp} is the apparent pre-consolidation pressure on the reference time line, ε_z^r is the "reference strain" at reference time line under σ'_z, and t_e is the equivalent time. t_e is equal to zero at the reference time line. Therefore, ε_{creep} in Eq.(1) corresponds to the strain from ε_z^r to ε_z. According to the EVP model (Yin and Graham 1994), varied t_e corresponds to a family of compression lines parallel to the reference time line, as shown in Fig.1. The relationship between visco-plastic strain rate $\dot{\varepsilon}_z^{vp}$ and t_e is unique. $\dot{\varepsilon}_z^{vp}$ can be calculated as:

$$\dot{\varepsilon}_z^{vp}=\frac{\partial \varepsilon_z}{\partial t}=\frac{\partial \varepsilon_z}{\partial t_e}=\frac{\psi_0}{Vt_0}\exp\left[\frac{-V\left(\varepsilon_z-\varepsilon_z^r\right)}{\psi_0\left(1-\frac{\varepsilon_z-\varepsilon_z^r}{\Delta\varepsilon_l}\right)}\right]\left(1-\frac{\varepsilon_z-\varepsilon_z^r}{\Delta\varepsilon_l}\right)^2 \tag{4}$$

2.2 3-D EVP model with creep limit

In the 3-D space, the mean effective normal stress $p^{'}$ and deviatoric stress q are defined as:

$$p^{'}=\frac{tr\left(\sigma_{ij}^{'}\right)}{3}=\frac{\sigma_{11}^{'}+\sigma_{22}^{'}+\sigma_{33}^{'}}{3} \tag{5a}$$

$$q=\sqrt{\frac{3}{2}\left(s_{ij}:s_{ij}\right)} \tag{5b}$$

$$s_{ij}=\sigma_{ij}^{'}-\delta_{ij}p^{'} \tag{5c}$$

$$\delta_{ij}=\begin{cases}1 & i=j\\ 0 & i\neq j\end{cases} \tag{5d}$$

With the associated flow rule, the flow direction of visco-plastic strain is controlled by the plastic potential function g, corresponding to the loading surface. In Yin et al. (2002), the loading surface contained two parts, one above the critical state line and one below the critical state line. Both of them were non-elliptical, with some independent parameters to describe the geometry. However, these parameters might be difficult to determine, especially for engineering applications. Besides, the equations for the loading surfaces are quite complicated, which increases the difficulty in differential equation derivation for implicit calculations in finite element modelling. In the meantime, some researchers adopted single elliptical loading surface based on the modified Cam-clay model, which also revealed good reasonability for various clayey soils (Zhou et al. 2005;

Grimstad et al. 2010; Yin et al. 2010; Freitas et al. 2012; Feng 2016; Chen et al. 2021a). Therefore, to simplify the problem without significantly reducing the accuracy, this study proposes to use the elliptical loading surface in the modified Cam-clay (MCC) model (Roscoe and Burland 1968):

$$g = \frac{q^2}{M^2 p^{'}} + p^{'} - p_m^{'} = 0 \tag{6}$$

in which M is the slope of critical state line in $p^{'} - q$ plane of MCC model, $p_m^{'}$ is the intersection point of surface $g = 0$ and the axis of $p^{'}$, which represents the "size" of loading surface, as shown in Fig.2.

Based on associated flow rule, the visco-plastic strain rate in the 3-D space is described as:

$$\dot{\varepsilon}_{ij}^{vp} = S \frac{\partial g}{\partial \sigma_{ij}^{'}} \tag{7}$$

where S is a scaling function representing the viscosity of the soil and $\frac{\partial g}{\partial \sigma_{ij}^{'}}$ is a tensor that controls the direction of deformation. It is considered that the volumetric visco-plastic strain rate is the same on the yielding surface, which means $\dot{\varepsilon}_v^{vp} = \dot{\varepsilon}_{vm}^{vp}$ (Vermeer and Neher 1999; Yin and Graham 1999; Yin et al. 2002; Feng 2016). According to Eq.(7), the value of S can be determined as:

$$S = \frac{\dot{\varepsilon}_v^{vp}}{\partial g / \partial p^{'}} = \frac{\dot{\varepsilon}_{vm}^{vp}}{\partial g / \partial p^{'}} \tag{8}$$

The relationship between ε_v and ε_{vm} is shown in Fig.2, which is two points on the same "elastic wall" and can be expressed in Eq.(9):

$$\varepsilon_{vm} = \varepsilon_v + \frac{\kappa}{V} \ln \frac{p_m^{'}}{p^{'}} \tag{9}$$

According to the 1-D EVP model, the value of $\dot{\varepsilon}_{vm}$ can be determined from:

$$\dot{\varepsilon}_{vm}^{vp} = \frac{\psi_0}{Vt_0} \exp\left[\frac{-V\left(\varepsilon_{vm} - \varepsilon_{vm}^{r}\right)}{\psi_0 \left(1 - \dfrac{\varepsilon_{vm} - \varepsilon_{vm}^{r}}{\Delta\varepsilon_l}\right)} \right] \left(1 - \frac{\varepsilon_{vm} - \varepsilon_{vm}^{r}}{\Delta\varepsilon_l}\right)^2 \tag{10}$$

where $\varepsilon_{vm}^{r} = \varepsilon_{v0} + \frac{\kappa}{V} \ln \frac{p_{mc}^{'}}{p_0^{'}} + \frac{\lambda}{V} \ln \frac{p_m^{'}}{p_{mc}^{'}}$ is the reference volumetric strain. The parameters can be calibrated from conventional 1-D or isotropic-stress consolidation tests. $p_{mc}^{'}$ is the size of "reference yielding surface" calculated by the pre-consolidation pressure $\sigma_{zp}^{'}$, as shown in the following equations:

$$p_{mc}^{'} = \frac{q_c^{\ 2}}{M^2 p_c^{'}} + p_c^{'} \tag{11a}$$

$$p_c^{'} = \left(\sigma_{zp}^{'} + 2K_0^{nc}\sigma_{zp}^{'}\right)/3 \tag{11b}$$

$$q_c = \sigma_{zp}^{'} - K_0^{nc}\sigma_{zp}^{'} \tag{11c}$$

where $K_0^{nc} = 1 - \sin\phi^{'} = 1 - \frac{3M}{6+M}$ is the coefficient of effective earth pressure at normal consolidation state.

3 Fully coupled finite element simulations for two embankments in PLAXIS 2D

3.1 Brief introduction to the algorithm for FE simulations

Using Eqs. (7) to (11), the visco-plastic strain rate of an element of soils under any stress-strain state can be calculated. The overall strain rate is calculated by:

$$\dot{\varepsilon}_{ij} = \dot{\varepsilon}_{ij}^{e} + \dot{\varepsilon}_{ij}^{vp} = \left(\frac{1}{2G^e}\dot{s}_{ij} + \frac{p^{'}}{3K^e}\dot{\delta}_{ij}\right) + S\frac{\partial g}{\partial \sigma_{ij}^{'}} \tag{12}$$

where $\dot{\varepsilon}_{ij}^{e}$ is the elastic strain rate calculated by the generalized Hooke's law, K^e is the elastic bulk modulus and G^e is the elastic shear modulus. K^e and G^e are calculated using the slope of instant time line κ and Poisson's ratio μ, as shown in Eq.(13):

$$K^e = \frac{1}{\partial \varepsilon_v^e / \partial p^{'}} = \frac{1}{\partial\left(\frac{\kappa}{V}\ln\frac{p^{'}}{p_0^{'}}\right)/\partial p^{'}} = \frac{Vp^{'}}{\kappa} \tag{13a}$$

$$G^e = \frac{3(1-2\mu)K^e}{2(1+\mu)} \tag{13b}$$

In the FE method, the mechanical behaviour can be determined using the Newton-Raphson's method and Euler's time iteration scheme in each small time-step (Feng et al. 2014; Li and Yin 2020). The vector of effective stress increment during a time-step is expressed by Eq.(14):

$$\Delta\boldsymbol{\sigma} = \mathbf{D}:\Delta\boldsymbol{\varepsilon}^e = \mathbf{D}:\left(\Delta\boldsymbol{\varepsilon} - \Delta\boldsymbol{\varepsilon}^{vp}\right) \tag{14}$$

The visco-plastic strain increment $\Delta\boldsymbol{\varepsilon}^{vp}$ is calculated by Euler time iteration scheme:

$$\Delta\boldsymbol{\varepsilon}^{vp,n} = \Delta t \cdot \left[(1-\theta)\cdot\dot{\boldsymbol{\varepsilon}}^{vp,n} + \theta\cdot\dot{\boldsymbol{\varepsilon}}^{vp,n+1}\right] \tag{15}$$

where $\theta \in [0,1]$ is a factor for combining both explicit ($\theta = 0$) and implicit ($\theta = 1$) methods, n represents the numbering of time step and Δt is the size of time step. Eqs.(14) and (15) are solved with Newton-Raphson's iteration:

$$\begin{cases} \boldsymbol{\sigma}^{n+1} = \boldsymbol{\sigma}^i + d\boldsymbol{\sigma}^i \\ \dot{\boldsymbol{\varepsilon}}^{vp,n+1} = \dot{\boldsymbol{\varepsilon}}^{vp,i} + \dfrac{\partial\dot{\boldsymbol{\varepsilon}}^{vp,i}}{\partial\boldsymbol{\sigma}} d\boldsymbol{\sigma} \end{cases} \tag{16}$$

where $\boldsymbol{\sigma}^i$ represents the updated stress and $\left|d\boldsymbol{\sigma}^i\right|$ is the residual at the iteration step which forces the iteration to stop when it is smaller enough.

The constitutive model is encoded into a dynamic link library (*.dll*) with FORTRAN language for application in the finite element program PLAXIS (2015). At each calculation step of each node, the current soil state (*e.g.* effective stress vector, strain vector and void ratio) and trial strain increment will be input into the functions defined in the *.dll* to produce a new stress vector for the next global iteration of the numerical model. The hydraulic behaviours are solved with Biot's 3-D consolidation equations. In this way, the stress-strain relationship is fully coupled with hydraulic behaviours by iteration algorithm.

3.2 Soil profiles and soil parameters for the Malaysian test embankments

In order to study the performance of highway embankments on Malaysian marine clay, Malaysian Highway Authority directed construction of several full-scale test embankments from1988 to 1989 (MHA 1989a, b). For comparison, there are two embankments (Scheme 3/2 and 6/6) directly built on the soft soils without measures of soil improvements (*e.g.* vertical drains), which have been monitored for a long time. The stratum under the test embankments contained multiple-layered marine soft soils, as shown in Fig.3. Details of the soil properties are listed in Table 1. The designed filling height is 3 m for Scheme 3/2 and 6 m for Scheme 6/6. Since the completion of construction in September 1989, the vertical and horizontal displacements and excess pore pressure at different depths and positions have been monitored by surface settlement makers, rod settlement gauges, inclinometers and pneumatic piezometers. Obviously, these cases contain multi-layered soft soil ground, multi-staged loading history, long-term monitoring and obvious plane-strain features, which are very suitable for verification of the proposed methods and model.

There is a crust cover with a thickness of 1.5 to 2.0 m underneath the fills. The crust mainly consists of weathered dark brown clay with roots and other materials. The average water content is around 60% and compressibility is relatively small. Laboratory studies on specimens from the crust layer demonstrated a pre-consolidation pressure σ'_{zp} of around 110 kPa. As the permeability data is yet unavailable, permeability of the adjacent clay will be used for the crust in this study.

The second layer is a soft marine clay with olive green colour, containing thin and discontinuous sand partings and slight organic components such as roots and leaves. This layer, named upper clay layer, has an average thickness of around 5 m. The soil parameters are found more uniform compared with the crust. However, test results on samples from the upper 2.5 m of this layer exhibit high uncertainty, possibly due to the structure effect and soil disturbance. For example, the initial water content, OCR and compressibility of the upper parts are also obviously higher than the lower parts. Therefore, it is necessary to divide the "upper clay" into two layers, namely "upper clay 1" and "upper clay 2" with thickness of 2.5 m for each. Considering the differences of initial void ratio e, the permeability of upper clay 1 should be modified using the following equation:

$$\log\frac{k_{v1}}{k_{v2}} = \frac{e_1 - e_2}{C_k} \tag{17}$$

where C_k is the permeability index and is assumed to be 0.5 in this study (Tavenas et al. 1983).

The third layer is a sandy silty clay layer of 1.6 m and the fourth is a lower clay layer of 9.2 m. The water content generally ranges from 50% to 70%. Below these layers follows a thin layer of peat and a stiff sandy clay layer. A layer of fine silty sand is located at the bottom.

All soil layers except the sand layer and the fill material are simulated using the nonlinear 3-D EVP model. In the EVP model, the value of pre-consolidation pressure σ'_{zp} is important in determination of the visco-plastic strain rate. According to the test results, the depth-dependency of σ'_{zp} is significant. Therefore, σ'_{zp} for each soil layer is defined using the concept of "pre-over-consolidation pressure (POP)", calculated by $\mathrm{POP} = \sigma'_{zp} - \sigma'_{z0}$, where σ'_{z0} is the initial in-situ effective stress. The usage of constant POP forms a piecewise linear distribution of σ'_{zp} with depth, as indicated in Fig.4. The values of compression index $\frac{C_c}{V}$ $(C_c = \lambda \ln 10)$ at different layers is shown in Fig.5. The values of unloading-reloading index κ were not reported in MHA's reports (MHA 1989a,b). Therefore, a proper value of $\kappa = 0.1\lambda$ is used in the simulations (Magnan and Katan 1989; Balasubramaniam et al. 2007). The secondary consolidation coefficient C_α of soils from different depth is measured under different vertical stress, which varied from 0.01 to 0.025. A constant creep coefficient $\psi_0 = \frac{C_\alpha}{\ln 10}$ with the averaged value of C_α is adopted in this study. Due to lack of long-term oedometer data, creep limit $\Delta\varepsilon_l = \frac{e}{1+e_0}$ is used in this study, which is the upper bound of $\Delta\varepsilon_l$. All parameters are selected based on the suggested or reported values by MHA (1989a,b).

3.3 Results of FE simulations

FE simulations are carried out for a cross-section of the embankment in PLAXIS 2D using the plane strain model, since the longitudinal deformation for a road embankment can be neglected. The numerical model of two embankments, Scheme 3/2 and 6/6, are shown in Fig.3. The construction is a multi-staged filling process, which can be described by the measured thickness of fill materials, as shown in Fig.6.

Fig.7 presents the settlement curves of the two embankments by FE simulations at different instrumentation points. “S” represents rod settlement gauge buried on the natural surface of the crust layer, while “SM” represents surface markers installed on the surface of the fill after completion of construction. With the parameters determined in the previous section, the simulation results fit well with the monitored results, especially the settlement measured by the surface markers.

Fig.8 shows the comparisons between calculated excess pore water pressure in the middle of marine clay with measured data by piezometers. In general, the simulated results are quite close to the monitored results. However, the quality of monitored pore water pressure is still a concern since the fluctuation of data is obvious, especially after a long period in service, which may explain the discrepancy between simulated results and measured data after a long time.

Fig.9 shows the lateral displacement at different depths and times from FE simulations and in-situ measurements by inclinometers installed in the soils. The simulation results for Scheme 3/2 are reliable, while the results for Scheme 6/6 are less accurate. One possible reason is that the inclinometer of Scheme 6/6 was installed inside the construction area, which could be disturbed by the filling process. For both embankments, lateral deformation is significant, especially at the top 10 meters from the ground surface. The largest lateral deformation tends to occur in the upper marine clay layers in which the volume compressibility and vertical strain are very high.

4 Parametric studies in FE simulations with the nonlinear 3-D EVP model

4.1 Influence of Compressibility

As reported by MHA (1989a), the compression index C_c of tested soil samples is found to have a discrete distribution within a certain range with high uncertainty, especially for the upper clay, as shown in Fig.5. Although the mean values of test data are adopted in Table 1, it is necessary to discuss the variations of results caused by different compressibility. In this sub-section, two additional cases are studied. In the first case, the upper bound of C_c for each layer is used in FE analysis. In the second case, the lower bound of C_c for each layer is used. C_r is 10% of C_c for all cases. Other parameters are kept unchanged from Table 1.

Calculated settlements at S5 for the two cases are shown in Fig.10, compared with measured data. The results indicate significant variations between the two sets of compressibility indices. The differences of final settlement at 3000 days between upper bound and lower bound of compressibility are around 0.2 m for Scheme 3/2 and 0.4 m for Scheme 6/6. The differences gradually increase with time due to the consolidation of soils. The results imply that despite of bad quality of measured data, using mean values of compressibility seems to be the optimal solution to this issue.

4.2 Influence of Creep Parameters

Creep parameters have significant effects on the time-dependent stress-strain behaviour of soft soils. For the test embankments, one-dimensional creep tests were conducted in laboratory to provide the secondary consolidation coefficient C_α ($C_\alpha = \psi_0 \ln 10$) under different effective stresses using the conventional fitting method $C_\alpha = \dfrac{\Delta e}{\Delta \log t}$. The values of C_α provided in MHA (1989a) are found discrete, with an upper bound of around 0.025 for the clayey soils. Due to nonlinear creep behaviour of clayey soils (Yin 1999), the creep coefficient is slightly decreased with vertical effective stress. Following this principle, the average creep coefficient of 0.015 considering the final surcharge loading is selected as in Table 1. In this parametric study, C_α is increased to its upper bound (*i.e.* 0.025) for all soil layers except the sandy clay layer and the sand layer. Another important parameter for the EVP model is the creep limit $\Delta\varepsilon_l$, which requires curve fitting from long-term oedometer tests. It is reported that for some of the marine soils, the values of creep limit roughly range from 0.03 to 0.06 (Yin 1999; Feng et al. 2017; Chen et al. 2021a). In this parametric study, one case with $\Delta\varepsilon_l = 0.05$ and another case with $\Delta\varepsilon_l = 1000$ are used for comparisons with $\Delta\varepsilon_l = \dfrac{e_0}{1+e_0}$ in Table 1. For $\Delta\varepsilon_l = 1000$, Eq.(1) is very close to the conventional linear creep model $\varepsilon_{creep} = \dfrac{\psi_0}{V}\ln\left(\dfrac{t+t_0}{t_0}\right)$ by Yin and Graham (1989).

Fig.11 shows the calculated settlements at S5 with different values of creep parameters. It can be seen that C_α has a significant influence on the long-term settlements. With $C_\alpha = 0.025$ for the soft clayey layers, the final settlements in 30 years are increased by around 0.25 m for both Scheme 3/2 and Scheme 6/6. In Scheme 3/2, it can be found that settlements are severely overestimated with $C_\alpha = 0.025$ even in the first several years. However, the influence of $\Delta\varepsilon_l$ is relatively minor, especially in the earlier phase. After 1000 days, the settlement with $\Delta\varepsilon_l = 0.05$ becomes visibly smaller than the other cases, while the case with $\Delta\varepsilon_l = \dfrac{e_0}{1+e_0}$ is still close to $\Delta\varepsilon_l = 1000$. Such results suggested that the value of $\Delta\varepsilon_l$ does influence the prediction results, but only for long-term prediction for post-construction settlement. To improve the accuracy of prediction, $\Delta\varepsilon_l$ should be measured in long-term oedometer tests in laboratory (Yin 1999), rather than be determined by $\Delta\varepsilon_l = \dfrac{e_0}{1+e_0}$.

4.3 Influence of Updating Static Water Pressure

The FE analysis on the embankments is conducted with the option of "update water pressure" in PLAXIS. With this option, the mesh of the FE model, static porewater pressure and effective stresses are updated with time with consideration of soil deformation, which enables more precise predictions under large deformation in the long term. Fig.12 presents the calculated settlement curves with and without updating static water pressure during the FE analysis. According to the results, the severe overestimation of settlements will occur without updating static water pressure. The reason is that with the continuous settlement of embankments into the groundwater level, the effective loading will be reduced by the buoyancy of water. Therefore, it is necessary to consider this option during the consolidation analysis.

5 An improved simplified Hypothesis B methods for calculating consolidation settlements at embankment centre with comparisons with measured data

5.1 Improved simplified Hypothesis B method considering nonlinear creep for 1-D consolidation settlement calculations

As shown in previous sections, FE method can be used to simulate the fully coupled and 2-D behaviour of an embankment through meshing and iteration techniques in a computer program. Due to the possible convergence difficulties of FE methods, in some cases, handy calculations based on certain assumptions are still widely adopted for simplified predictions of settlement and cross-checking for FE simulations. For 1-D consolidation settlement analysis of a thick layer of soils without creep, Terzaghi's consolidation theory is the most classical and widely adopted method. Based on Terzaghi's theory, researchers have developed different theoretical and semi-empirical methods to calculate the consolidation settlements of soils subjected to multi-layered stratum, multi-staged and time-dependent loading and vertical drains (Zhu and Yin 2005; Chen et al. 2005; Walker et al. 2009; Yin and Zhu 2020). In these solutions, iteration algorithm is not required, and convergence is no longer a problem. To consider creep deformation, the simplified Hypothesis B method (Yin and Feng 2017; Feng and Yin 2017; Yin and Zhu 2020) has been proposed for soft clayey soils based on existing analytical solutions for primary consolidation and 1-D EVP model for creep analysis.

Hypothesis B is a theory advocating that viscous compression should be considered during the "primary consolidation", opposed to Hypothesis A that the creep only occurs after end of primary consolidation (Ladd et al. 1977; Mesri and Godlewski 1977). Hypothesis B has been widely accepted and implemented in most fully coupled analysis methods (Leroueil et al. 1985; Yin and Graham 1989; Vermeer and Neher 1999; Hinchberger and Rowe 2005; Kellen et al. 2008; Degago et al. 2011; Watabe et al. 2012; Grimstad et al. 2017). Despite of this, when finite element software is not adopted, many engineers and construction codes still turn back to Hypothesis A because it can be easily achieved by hand calculation. There exists an obvious lag between engineering practice and research development.

The intensive of simplified Hypothesis B method is to avoid iterations and meshing in the fully coupled consolidation analysis and improve the practicality of Hypothesis B. In Chen et al. (2021b)'s new simplified Hypothesis B method, the total settlement of multi-layered clayey soils is calculated as:

$$S_{totalB} = S_{primary} + S_{creep} = \sum_{j=1}^{j=n} U_j S_{fj} + \sum_{j=1}^{j=n} [\alpha U_j S_{creep,fj} + (1-\alpha U_j) S_{creep,dj}] \quad \text{for all } t \geq t_0 \;\; (t \geq t_{EOP,field} \text{ for } S_{creep,dj}) \tag{18}$$

where S_{totalB} represents the total settlement with time, j denotes numbering of soil layer, U_j is the degree of consolidation for the *j*-layer, α is an empirical parameters ranging from 0 to 1 to considering creep delayed by primary consolidation. Eq. (18) can be reduced to Hypothesis A by setting $\alpha = 0$. Details of the values of α can be found in Yin and Zhu (2020) and Chen et al. (2021b). $\alpha = 0.8$ is frequently used and found effective for general cases. t_0 is the reference time (*e.g.* one day). $t_{EOP,field}$ is the time needed for "end of primary consolidation (EOP)" of the soil layer, which can be calculated using Walker et al. (2009)'s spectral method for multi-layered soil consolidation problem. S_f equals to the "primary consolidation settlement" under the targeted increment of loading without considering any creep strain. The value of S_f for each layer under each loading is directly determined from the $\varepsilon_z - \log\sigma_z^{'}$ curve according to its stress history, as shown in Fig.13. Considering the nonlinear 1-D EVP model, the calculation of instant creep settlement $S_{creep,f}$ and delayed creep settlement $S_{creep,d}$ for each layer should be derived as Eqs. (19a) and (19b):

$$S_{creep,f} = H_j \left[\frac{\frac{\psi_0}{V} \ln\left(\frac{t_e + t_0}{t_0}\right)}{1 + \frac{\psi_0}{V\Delta\varepsilon_l} \ln\left(\frac{t_e + t_0}{t_0}\right)} - \left(\varepsilon_{zf} - \varepsilon_{zf}^r\right) \right], \text{ for } t > t_0 \tag{19a}$$

$$S_{creep,d} = H_j \left[\frac{\frac{\psi_0}{V} \ln\left(\frac{t_e + t_0}{t_{EOP,field}}\right)}{1 + \frac{\psi_0}{V\Delta\varepsilon_l} \ln\left(\frac{t_e + t_0}{t_{EOP,field}}\right)} - \left(\varepsilon_{zf} - \varepsilon_{zf}^r\right) \right], \text{ for } t > t_{EOP,field} \tag{19b}$$

where $t_e = t_{ei} + t - t_c / 2$ is the equivalent time in the EVP model, t is the total time of the consolidation stage, t_c is the construction time, ε_{zf} is the final strain under stress $\sigma_{zf}^{'}$ without considering creep, ε_{zf}^r is the reference strain located at the reference time line under $\sigma_{zf}^{'}$, and t_{ei}

is the equivalent time at the final state of stress σ'_{zf} and strain ε_{zf}, as shown in Fig.13. The value of final strain state ε_{zf} can be calculated by Eq. (20):

$$\varepsilon_{zf} = \max\left[\varepsilon_{z\_total(\text{last stage})} + \frac{\kappa}{V}\ln\frac{\sigma'_{zf(i)}}{\sigma'_{zf(i-1)}}, \varepsilon_{zp} + \frac{\lambda}{V}\ln\frac{\sigma'_{zf(i)}}{\sigma'_{zp}}\right] \tag{20}$$

where $\varepsilon_{z\_total(\text{last stage})} = \varepsilon_{z0} + \sum_{\text{past stages}} \left(S_f + S_{creep}\right)/H_j$ is the accumulated strain from previous stages. When $\varepsilon_{z\_total(\text{last stage})} + \frac{\kappa}{V}\ln\frac{\sigma'_{zf}}{\sigma'_{zf(\text{last stage})}} < \varepsilon_{zp} + \frac{\lambda}{V}\ln\frac{\sigma'_{zf}}{\sigma'_{zp}}$, the final state is under normal consolidation and t_{ei} is equal to zero. Otherwise, the soil layer is under over-consolidation state and the value of t_{ei} can be calculated as follows:

$$\begin{aligned} t_{ei} &= \exp\left[\frac{\varepsilon_{zf} - \varepsilon_z^r}{\frac{\psi_0}{V}\left(1 - \frac{\varepsilon_{zf} - \varepsilon_z^r}{\Delta\varepsilon_l}\right)}\right] t_0 - t_0 \\ &= \exp\left\{\frac{\left[\left(\varepsilon_{zf} - \varepsilon_{zp}\right) - \frac{\lambda}{V}\log\left(\frac{\sigma'_{zf}}{\sigma'_{zp}}\right)\right]}{\frac{\psi_0}{V}\left(1 - \frac{\left(\varepsilon_{zf} - \varepsilon_{zp}\right) - \frac{\lambda}{V}\log\left(\frac{\sigma'_{zf}}{\sigma'_{zp}}\right)}{\Delta\varepsilon_l}\right)}\right\} t_0 - t_0, \quad \text{for } \left(\varepsilon_{zf} - \varepsilon_z^r\right) < \Delta\varepsilon_L \end{aligned} \tag{21}$$

In Eq. (21), when $\left(\varepsilon_{zf} - \varepsilon_z^r\right) > \Delta\varepsilon_l$, the stress-strain state of soil is below the limit time line, so the value of t_{ei} is $+\infty$ and $S_{creep,f} = S_{creep,d} = 0$. The major procedures of simplified Hypothesis

B method are revealed in Fig.13. More details about the simplified Hypothesis B method can be found in Chen et al. (2021b) and Yin and Zhu (2020).

5.2 Modification of the simplified Hypothesis B method with considerations of stress reduction underneath 2-D embankments

Under multi-staged loading, the total settlement calculated by Eq.(18) from each loading stage can be superposed as the accumulated total settlement, as shown in Fig.13. For embankments with an unloading stage, the superposition might not be reasonable since the accumulated plastic deformation of soils is dependent of the actual consolidation time.

Besides, this method is only limited to 1-D compression, which may differ from the field conditions, especially for road embankments constructed on thick layers of clay, including the cases in this study. Although it can be assumed that the centerline of the embankment is still subjected to 1-D compression and vertical drainage, the stress reduction caused by stress diffusion cannot be neglected. In addition, this method has not considered the effects of buoyancy due to the gradual settlement of embankments into the original ground level, by which the actual surcharge will be reduced with time. Therefore, 1-D simplified methods should be adjusted to simulate the real settlement under the field condition.

(1) Effects of additional stress diffusion

For a finite-length load applied on the infinite soil ground, the vertical stress will decrease with depth due to the diffusion of additional stress. Flamant (1892) developed an elastic solution for stress distribution with depth for the case of a strip load applied on a semi-infinite half-space of homogeneous isotropic soils. Flamant’s solution can be used to calculate the stress distribution under a strip loading by integral (Gong and Xie 2014). Further to consider the geometry of embankments, Osterberg (1957) developed a series of solutions for external loadings in the shape of triangle, strip, and embankment (trapezoid) and provided influence charts for engineers' use. However, as noticed by previous researchers (Schmertmann 2005; Wang et al. 2019), both Flamant's solution and Osterberg's charts are elastic solutions and should not be directly adopted in settlement analysis for soft clayey soils, since the stress-strain behaviours of soft soils are much different from elastic materials. Besides, the existing elastic solutions usually require chart method, which is not convenient and time-consuming. A new formulation for vertical stress reduction based on the FE simulations will be more suitable. Considering the boundary conditions that $\lim_{\frac{z}{B}\to\infty} \Delta\sigma'_{zf}\left(\frac{z}{B}\right)=0$ and $\Delta\sigma'_{zf}(0)=Q'$, the simplest mathematical model of additional stress distribution can be assumed as the following hyperbolic function:

$$\Delta\sigma'_{zf}(z)=\frac{Q'}{1+z/B} \tag{22}$$

where $\Delta\sigma'_{zf}$ is the additional vertical stress, Q' is the loading applied on the surface, z is the depth, B is the width at the middle of the embankment, which is simplified as s strip load, as shown in Fig.14. The larger B, the closer to 1-D case. For a multi-staged constructed embankment, different values of B will be considered independently for each stage of Q'. In this way, the influence of special geometry of embankment, for example, Scheme 6/6 in this study, can be taken into account.

Fig.14 presents the distribution of total additional vertical stress at the center with depth by FE simulations, elastic solution and Eq.(22). The ratio of $\frac{\Delta\sigma'_{zf}}{Q'}$ for Scheme 6/6 was calculated by $\frac{\Delta\sigma'_{zf1}+\Delta\sigma'_{zf2}+\Delta\sigma'_{zf3}}{Q'_1+Q'_2+Q'_3}$ from three independently analyzed trapezoids. It can be found that the

$\frac{\Delta\sigma'_{zf}}{Q'}$ for two embankments exhibits decreasing trend with depth, in which $\frac{\Delta\sigma'_{zf}}{Q'}$ for Scheme 3/2 decreased more sharply due to the smaller length. Prediction results by the proposed method in this study are fairly close to the results by FE simulation, while elastic solutions by Flamant and Osterberg tend to overestimate $\frac{\Delta\sigma'_{zf}}{Q'}$ at different depths. Therefore, Eq.(22) is considered effective to be used in the simplified hypothesis B method. Compared with the 1-D simplified method (Chen et al. 2021b), only one additional parameter, *B*, is introduced in the updated equations.

It should be noted that this method only serves as a simplified way for correcting the 1-D settlement curves at the centre of embankments. The deformations caused by rotations and torsion are neglected. The influences of plastic deformation on the stress diffusion mode during the superposition of multi-stage loadings are not considered either. Therefore, this method does not apply to embankments with large horizontal and shear strains, as well as locations away from the centre line.

(2) Effects of buoyancy

With the settlement of soils, part of the surcharge from the embankment will be compensated by the buoyancy force of groundwater. In the FEM analysis, the buoyancy effect is considered by updating water pressure for each calculation step. In simplified methods, the buoyancy effect may be calculated with a simple approach. Considering a soil layer subjected to an initial vertical surcharge Q, the actual effective surcharge Q' can be estimated as:

$$Q' = Q - \gamma_w S' \tag{23}$$

where $S^{'}$ is the total actual settlement of the soil layer, γ_w is the unit weight of water. The actual consolidation settlement can be approximated as $S^{'} = UHm_v Q^{'}$, where H is the initial thickness of the soil. Therefore, substituting Eq. (23) to $S^{'} = UHm_v Q^{'}$, we have:

$$S^{'} = UHm_v \left(Q - \gamma_w S^{'} \right) \tag{24}$$

Eq. (24) can be re-organized as:

$$S^{'} = \frac{UHm_v Q}{\left(1 + UHm_v \gamma_w\right)} \tag{25}$$

Finally, substituting $UHm_v Q = S$ into Eq. (25), the following expression is obtained:

$$S^{'} = \frac{S}{1 + S\gamma_w / Q} \tag{26}$$

Therefore, the actual settlement $S^{'}$ considering buoyancy can be directly adjusted from the original calculated settlement S without buoyancy correction. For multi-layered and multi-staged cases, it is assumed that Eq.(24) is still effective, to avoid the iterations and integration of stress-strain relations at different layers. Finally, the time-dependent settlement by Eq.(18) should be corrected as:

$$S^{'}\left(t\right) = \sum_i \frac{S_i\left(t\right)}{1 + S_i\left(t\right)\gamma_w / Q_i} \tag{27}$$

5.3 Calculation results by the 2-D simplified Hypothesis B method compared with FE simulation and in-situ measurement

All parameters are kept the same as in the FE simulation. The compressibility m_v for each layer is calculated by $m_v = \dfrac{S_f}{H_j \Delta\sigma_{zf}}$. The soil parameters are input to the Walker et al. (2009)'s spectral method for calculations of U_j and then S_{totalB} by Eq.(18) in each stage. The empirical factor $\alpha = 0.8$ in Eq.(18) is used for analysis. For comparison, a case with $\alpha = 0$ (*i.e.,* Hypothesis A method) is studied.

Using the improved simplified Hypothesis B method, the settlement curves at the centre of embankments can be obtained. Fig.16 shows the comparisons between the calculation results by FE method (2-D FEM), simplified Hypothesis B method with modifications for stress diffusion and buoyancy (new SBM), original simplified Hypothesis B method without modifications (original 1-D SBM), Hypothesis A method, and measured data. According to Fig.16, the results by the new SBM agree well with the FE simulations and in-situ measurements. Results from original SBM show obvious overestimation compared with improved SBM and FEM. Results from Hypothesis A, in which creep only occurs after the end of primary consolidation, exhibit underestimations of settlement. Therefore, the proposed simple method with considerations of Hypothesis B, 2-D stress diffusion and buoyancy effect is effective for embankment analysis.

According to these results, the proposed simple method is promising in predicting the settlements of the embankments in both convenience and accuracy. It can be done in an Excel spreadsheet and does not require solving complicated equations for force equilibrium and 3-D consolidations or solution charts. However, since the equations are empirically based, further examinations for more general cases based on public database are necessary. The current method is only applicable to the settlements of centre lines under the embankments with small horizontal and shear strain and without an unloading stage. For further studies, the effects of deviatoric stress and shear stress, displacements at different positions and directions, and the unloading-reloading stages should be taken into consideration.

6 Conclusions

To study the long-term and time-dependent consolidation settlement of embankments, a nonlinear three-dimensional elastic visco-plastic (3-D EVP) model with a creep limit is improved and encoded in both finite element program and simple method. Simulations on two test embankments constructed on multi-layered Malaysian marine soft soils with a complicated construction history were conducted with the EVP model. The results of FE simulations are compared with in-situ measured data for verifying the suitability and accuracy of the nonlinear 3-D EVP model. Parametric studies on the parametric optimization and modelling techniques are conducted and presented with discussions. An improved simplified Hypothesis B method is proposed with considerations of creep limit, 2-D effects in distribution of stress, and buoyancy effects for consolidation settlement analysis of the test embankments. This new improved simplified method is also verified with measured data and FE simulations. Based on the works presented above, several important conclusions can be summarized as follows:

(1) The nonlinear 3-D EVP model incorporating Yin (1999)'s nonlinear creep function and the modified Cam-Clay model is suitable and accurate for simulating time-dependent consolidation settlements of full-scale embankments on natural soft soils. The computed settlements, horizontal displacements, and excess pore water pressure dissipation are reliable and reasonable with comparisons to the in-situ measured data.

(2) The parametric studies reveal the importance of parameter selection in computational simulations. Generally, the use of mean values of soil parameters (*e.g.* C_c, C_r, C_α) is the optimal way for getting good modelling results.

(3) As for the long-term creep behaviour, $\Delta\varepsilon_l$ obtained from oedometer test is an important parameter, although assuming $\Delta\varepsilon_l = \frac{e_0}{1+e_0}$ is still acceptable in a relatively short course.

(4) The update of static water pressure in fully coupled FE analysis has a major influence on the simulation results. Without this option, the final settlements are severely overestimated.

(5) The Hypothesis A method and original simplified Hypothesis B method have obvious limitations in the prediction of consolidation settlements for the highway embankments.

(6) The improved simplified Hypothesis B method considering stress diffusion and buoyancy with two simple equations achieves reliable predictions compared with measured data and FE simulations. Further improvements are recommended to include the shear behaviour and the unloading-reloading behaviour of soils, towards a more rigorous yet easily-implemented approach beyond the simple superposition for multi-staged loading cases.

Acknowledgement

The work in this paper is supported by a Research Impact Fund (RIF) project (R5037-18), a Theme-based Research Scheme Fund (TRS) project (T22-502/18-R), and three General Research Fund (GRF) projects (PolyU 152179/18E; PolyU 152130/19E; PolyU 152100/20E) from Research Grants Council (RGC) of Hong Kong Special Administrative Region Government of China. The authors also acknowledge the financial supports from Research Institute for Sustainable Urban Development of The Hong Kong Polytechnic University and a grant ZDBS from The Hong Kong Polytechnic University.

References

Adachi, T., & Oka, F. (1982). Constitutive equations for normally consolidated clay based on elasto-viscoplasticity. *Soils and foundations*, *22*(4), 57-70.

Balasubramaniam, A. S., Huang, M., Bolton, M., Oh, E. Y. N., Bergado, D. T., & Phienwej, N. (2007). Interpretation and analysis of test embankments in soft clays with and without ground improvement. *Geotechnical Engineering*, *38*(3), 235.

Biot, M. A. (1956). General solutions of the equations of elasticity and consolidation for a porous material. *J. appl. Mech*, *23*(1), 91-96.

Borja, R. I., & Kavazanjian, E. (1985). A constitutive model for the stress–strain–time behaviour of ‘wet’ clays. *Geotechnique, 35(3),* 283-298

Brinkgreve, R. B. J., & Broere, W. (2015). PLAXIS 2D Reference Manual 2015. *Delft, Netherlands2010*.

Chen, R. P., Zhou, W. H., Wang, H. Z., & Chen, Y. M. (2005). One-dimensional nonlinear consolidation of multi-layered soil by differential quadrature method. *Computers and Geotechnics*, *32*(5), 358-369.

Chen, Z. J., Feng, W. Q., Yin, J. H. (2021a). Finite Element Simulations of Clayey Soil Ground with a Three-Dimensional Nonlinear Elastic Viscoplastic Model. In: Barla M., Di Donna A., Sterpi D. (eds) *Challenges and Innovations in Geomechanics. IACMAG 2021. Lecture Notes in Civil Engineering*, vol *125*. Springer, Cham. https://doi.org/10.1007/978-3-030-64514-4_34

Chen, Z. J., Feng, W. Q., & Yin, J. H. (2021b). A new simplified method for calculating short-term and long-term consolidation settlements of multi-layered soils considering creep limit. *Computers and Geotechnics*, 138, 104324.

Fatahi, B., Le, T. M., Le, M. Q., & Khabbaz, H. (2013). Soil creep effects on ground lateral deformation and pore water pressure under embankments. *Geomechanics and Geoengineering*, *8*(2), 107-124.

Feng, W. (2016). Experimental study and constitutive modelling of the time-dependent stress-strain behavior of soils. The Hong Kong Polytechnic University, Hong Kong.

Feng, W. Q., Lalit, B., Yin, Z. Y., & Yin, J. H. (2017). Long-term non-linear creep and swelling behavior of Hong Kong marine deposits in oedometer condition. *Computers and Geotechnics*, *84*, 1-15.

Feng, W. Q., Li, Y. L., Yin, J. H., & Yin, Z. Y. (2014). The numerical implementation of elastic visco-plastic model for soft clays. *Numerical Methods in Geotechnical Engineering*, 39.

Feng, W. Q., & Yin, J. H. (2017). A new simplified Hypothesis B method for calculating consolidation settlements of double soil layers exhibiting creep. *International Journal for Numerical and Analytical Methods in Geomechanics*, *41*(6), 899-917.

Feng, W. Q., Lalit, B., Yin, Z. Y., & Yin, J. H. (2017). Long-term non-linear creep and swelling behavior of Hong Kong marine deposits in oedometer condition. *Computers and Geotechnics*, *84*, 1-15.

Feng, W. Q., & Yin, J. H. (2018). A new simplified Hypothesis B method for calculating the consolidation settlement of ground improved by vertical drains. *International Journal for Numerical and Analytical Methods in Geomechanics*, *42*(2), 295-311.

Feng, W. Q., Yin, J. H., Chen, W. B., Tan, D. Y., & Wu, P. C. (2020). A new simplified method for calculating consolidation settlement of multi-layer soft soils with creep under multi-stage ramp loading. *Engineering Geology*, *264*, 105322.

Flamant, M. (1892). On the distribution of stresses in a two dimensional solid under transverse loading. *Acad. Sci., Paris, C. R. 114*, 1465–1468 (in French).

Freitas, T. M. B., Potts, D. M., & Zdravkovic, L. (2011). A time dependent constitutive model for soils with isotach viscosity. *Computers and Geotechnics*, *38*(6), 809-820.

Folkes, D. J., & Crooks, J. H. A. (1985). Effective stress paths and yielding in soft clays below embankments. *Canadian Geotechnical Journal*, *22*(3), 357-374.

Gong, X. N., & Xie, K. H. (2014). *Soil mechanics*. China Architecture & Building Press, Beijing

Graham, J., Crooks, J. H. A., & Bell, A. L. (1983). Time effects on the stress-strain behaviour of natural soft clays. *Géotechnique*, *33*(3), 327-340.

Grimstad, G., Degago, S. A., Nordal, S., & Karstunen, M. (2010). Modeling creep and rate effects in structured anisotropic soft clays. *Acta Geotechnica*, *5*(1), 69-81.

Hansbo, S., Jamiolkowski, M., & Kok, L. (1981). Consolidation by vertical drains. *Géotechnique*, *31*(1), 45-66.

Hinchberger, S. D., & Rowe, R. K. (1998). Modelling the rate-sensitive characteristics of the Gloucester foundation soil. *Canadian Geotechnical Journal*, *35*(5), 769-789.

Hinchberger, S. D., & Rowe, R. K. (2005). Evaluation of the predictive ability of two elastic-viscoplastic constitutive models. *Canadian Geotechnical Journal*, *42*(6), 1675-1694.

Kelln, C., Sharma, J., Hughes, D., & Graham, J. (2008). An improved elastic–viscoplastic soil model. *Canadian Geotechnical Journal*, *45*(10), 1356-1376.

Kutter, B. L., & Sathialingam, N. (1992). Elastic-viscoplastic modelling of the rate-dependent behaviour of clays. *Géotechnique*, *42*(3), 427-441.

Ladd, C. C., Foott, R., Ishihara, K., Schlosser, F., & Poulos, H. G. (1977). Stress deformation and strength characteristics. In *International Conference on Soil Mechanics and Foundation Engineering, 9th, 1977, Tokyo, Japan* (Vol. 2).

Lerouel, S., Kabbaj, M., Tavenas, F., & Bouchard, R. (1985). Stress-strain-strain rate relation for the compressibility of sensitive natural clays compressibility. *Geotechnique*, *35*(2), 159-180.

Li, J., & Yin, Z. Y. (2020). A modified cutting-plane time integration scheme with adaptive substepping for elasto-viscoplastic models. *International Journal for Numerical Methods in Engineering*, *121*(17), 3955-3978.

Loganathan, N., Balasubramaniam, A. S., & Bergado, D. T. (1993). Deformation analysis of embankments. *Journal of Geotechnical Engineering*, *119*(8), 1185-1206.

Magnan, J., & Kattan, A. (1989). Additional analysis and comments on the performance of Muar Flats trial embankment to failure. In *Int. Symp. on Trial Embankments on Malaysian Marine Clays* (pp. 11-1).

Malaysian Highway Authority (MHA). (1989a). *"Proceedings of the International Symposium on Trial Embankments on Malaysian Marine Clays"*, Kuala Lumpur, Malaysia. Volume 1. The Malaysian Highway Authority.

Malaysian Highway Authority (MHA). (1989b). *"Proceedings of the International Symposium on Trial Embankments on Malaysian Marine Clays"*, Kuala Lumpur, Malaysia. Volume 2. The Malaysian Highway Authority.

Mesri, G., & Godlewski, P. M. (1977). Time-and stress-compressibility interrelationship. *Journal of the geotechnical engineering division*, *103*(5), 417-430.

Osterberg, J. O. (1957). Influence Values for Vertical Stresses in a Semi-infinite Mass due to an Embankment Loading. In *Proc., 4th Int. Conf. Soil Mechanics Foundation Engineering*, 393–394.

Perzyna, P. (1963). The constitutive equations for rate sensitive plastic materials. *Quarterly of Applied Mathematics*, *20*(4), 321-332.

Poulos, H. G., Lee, C. Y., & Small, J. C. (1989). Prediction of embankment performance on Malaysian marine clays. In *Int. Symp. on Trial Embankments on Malaysian Marine Clays* (Vol. 3, pp. 22-30).

Roscoe, K., & Burland, J. B. (1968). On the generalized stress-strain behaviour of wet clay.

Schmertmann, J. H. (2005). Stress diffusion experiment in sand. *Journal of Geotechnical and Geoenvironmental Engineering*, *131*(1), 1-10.

Shi, X. S., Yin, J., Feng, W., & Chen, W. (2018). Creep coefficient of binary sand–bentonite mixtures in oedometer testing using mixture theory. *International Journal of Geomechanics*, *18*(12), 04018159.

Tavenas, F., Jean, P., Leblond, P., & Leroueil, S. (1983). The permeability of natural soft clays. Part II: Permeability characteristics. *Canadian Geotechnical Journal*, *20*(4), 645-660.

Terzaghi, K. (1943). *Theoretical soil mechanics*. Wiley, New York.

Vermeer, P. A., & Neher, H. P. (1999). A soft soil model that accounts for creep. *Beyond 2000 in computational geotechnics*, 249-261.

Walker, R., Indraratna, B., & Sivakugan, N. (2009). Vertical and radial consolidation analysis of multilayered soil using the spectral method. *Journal of Geotechnical and Geoenvironmental Engineering*, *135*(5), 657-663.

Wang, H., Zeng, L. L., Bian, X., & Hong, Z. S. (2019). Evaluation of vertical superimposed stress in subsoil induced by embankment loads. *International Journal of Geomechanics*, *19*(1), 04018182.

Yin, J. H., & Feng, W. Q. (2017). A new simplified method and its verification for calculation of consolidation settlement of a clayey soil with creep. *Canadian Geotechnical Journal*, *54*(3), 333-347.

Yin, J. H., & Graham, J. (1989). Viscous–elastic–plastic modelling of one-dimensional time-dependent behaviour of clays. *Canadian Geotechnical Journal*, *26*(2), 199-209.

Yin, J. H., & Graham, J. (1994). Equivalent times and one-dimensional elastic viscoplastic modelling of time-dependent stress–strain behaviour of clays. *Canadian Geotechnical Journal*, *31*(1), 42-52.

Yin, J. H., & Graham, J. (1999). Elastic viscoplastic modelling of the time-dependent stress-strain behaviour of soils. *Canadian Geotechnical Journal*, *36*(4), 736-745.

Yin, J. H. (1999). Non-linear creep of soils in oedometer tests. *Geotechnique*, *49*(5), 699-707.

Yin, J. H., Zhu, J. G., & Graham, J. (2002). A new elastic viscoplastic model for time-dependent behaviour of normally and overconsolidated clays: theory and verification. *Canadian Geotechnical Journal*, *39*(1), 157-173.

Yin, J. H., & Zhu, G. (2020). *Consolidation analyses of soils*. CRC Press, London.

Yin, Z. Y., Chang, C. S., Karstunen, M., & Hicher, P. Y. (2010). An anisotropic elastic–viscoplastic model for soft clays. *International Journal of Solids and Structures*, *47*(5), 665-677.

Zhu, G., & Yin, J. H. (2004). Consolidation analysis of soil with vertical and horizontal drainage under ramp loading considering smear effects. *Geotextiles and Geomembranes*, *22*(1-2), 63-74.

Zhou, C., Yin, J. H., Zhu, J. G., & Cheng, C. M. (2005). Elastic anisotropic viscoplastic modeling of the strain-rate-dependent stress–strain behavior of K 0-consolidated natural marine clays in triaxial shear tests. *International Journal of Geomechanics, 5*(3), 218-232.

List of Figure Captions

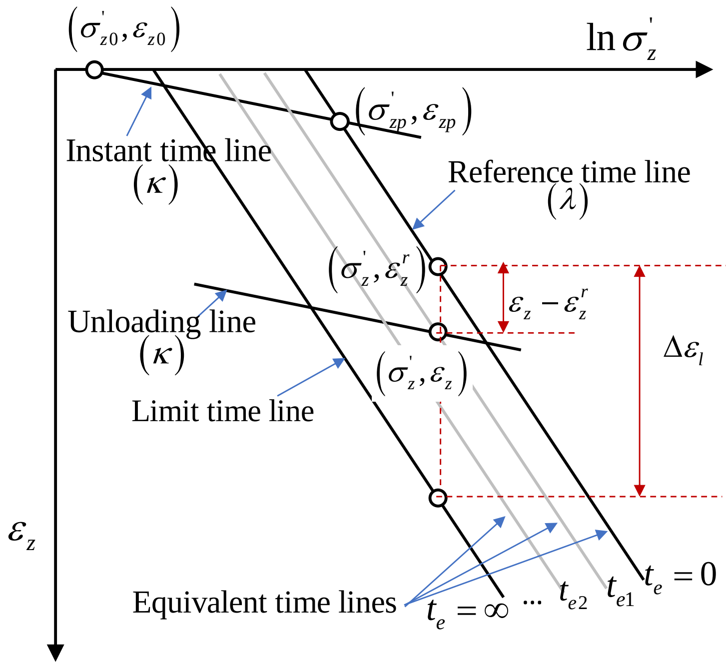

Fig.1. Schematic diagram of the 1-D EVP model

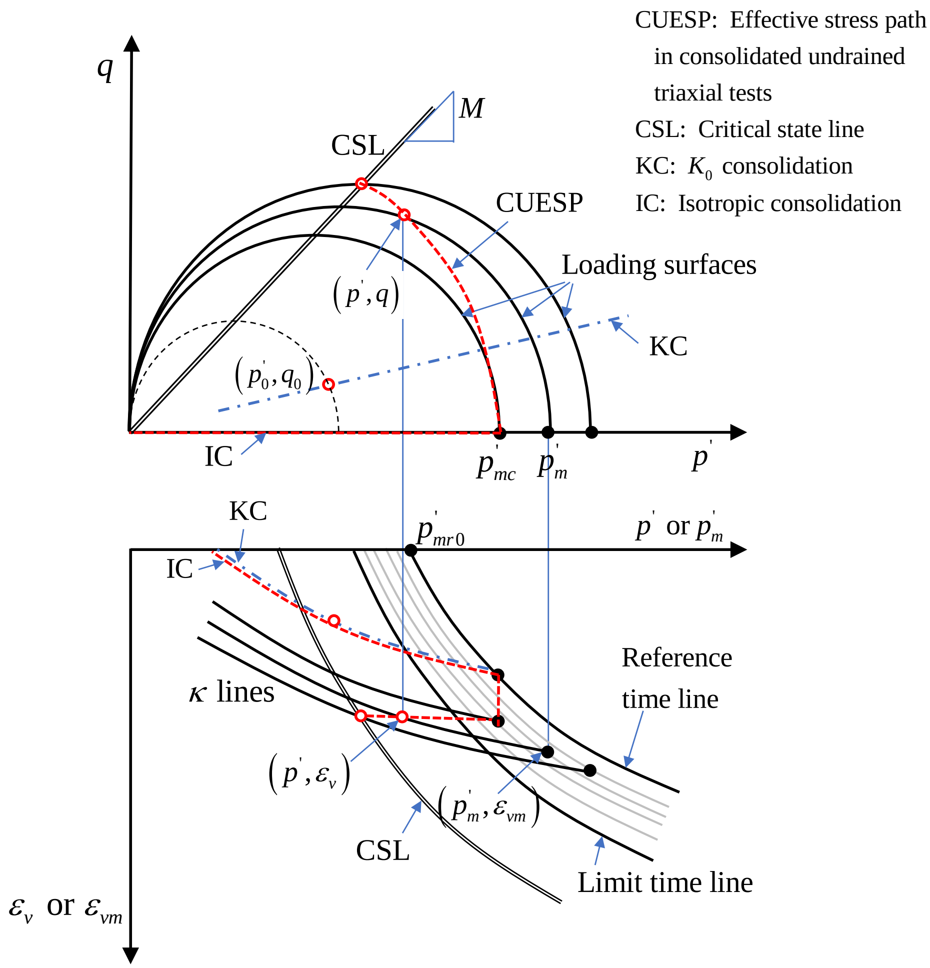

Fig.2. Schematic diagram of the 3-D EVP model

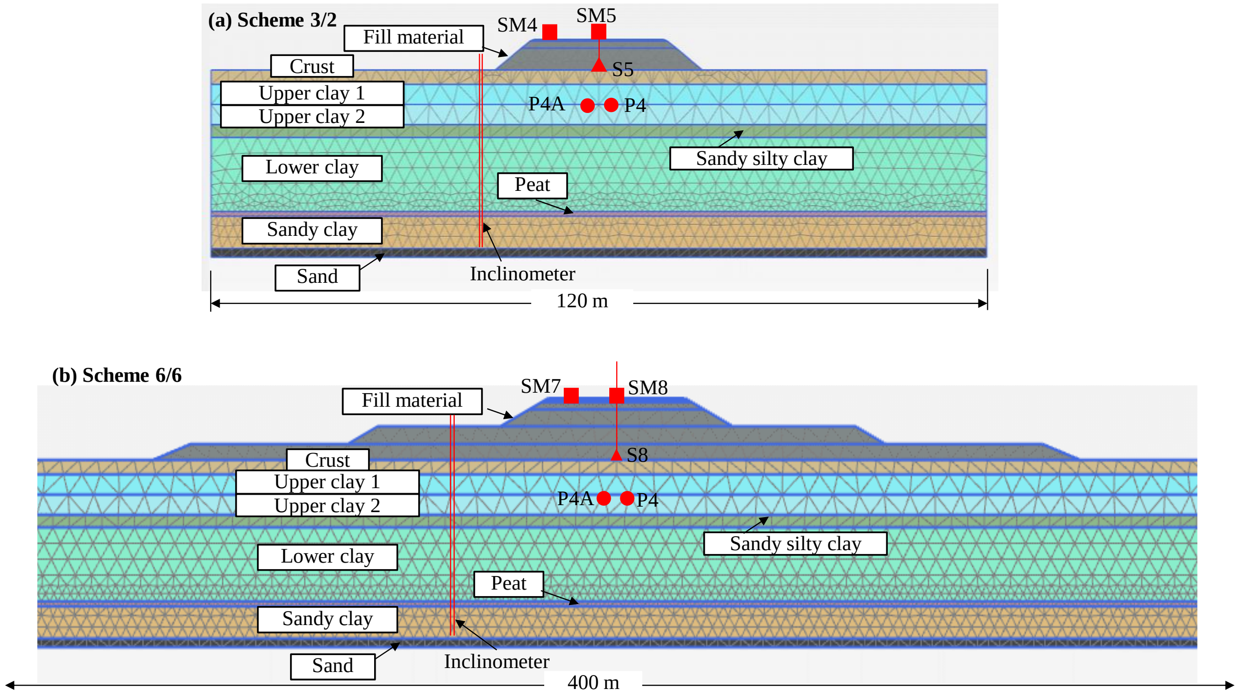

Fig.3. Profiles of the two embankments and their meshed numerical models

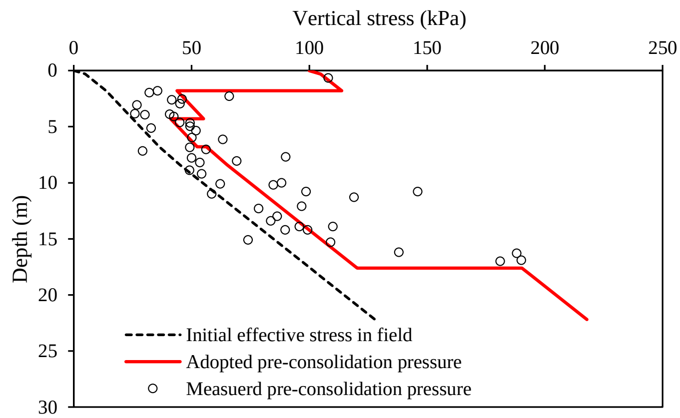

Fig.4. Initial effective stress and pre-consolidation pressure profiles of soils with depth (after MHA, 1989a)

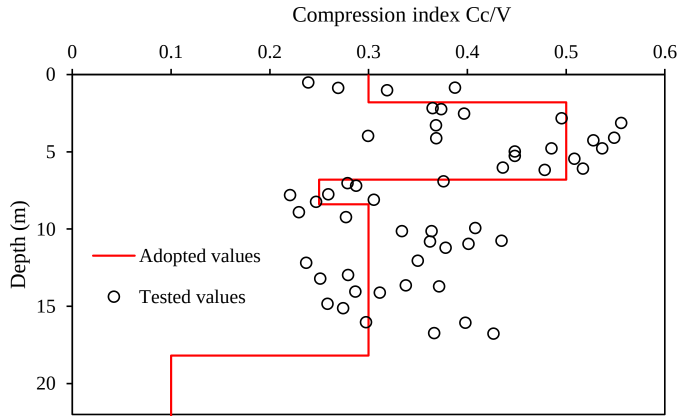

Fig.5. Compression index profile of soils with depth (after MHA, 1989a)

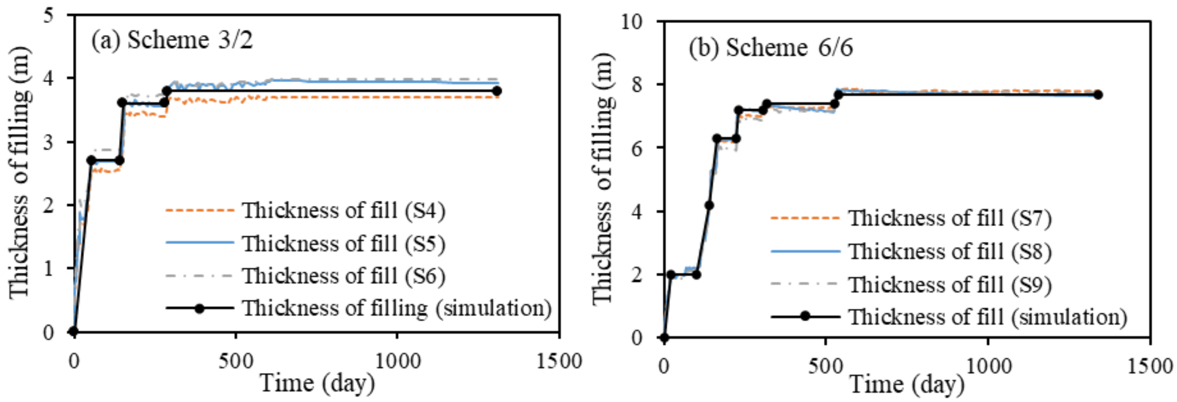

Fig.6. Thickness of fill with time at the center of embankments of Schemes 3/2 and 6/6

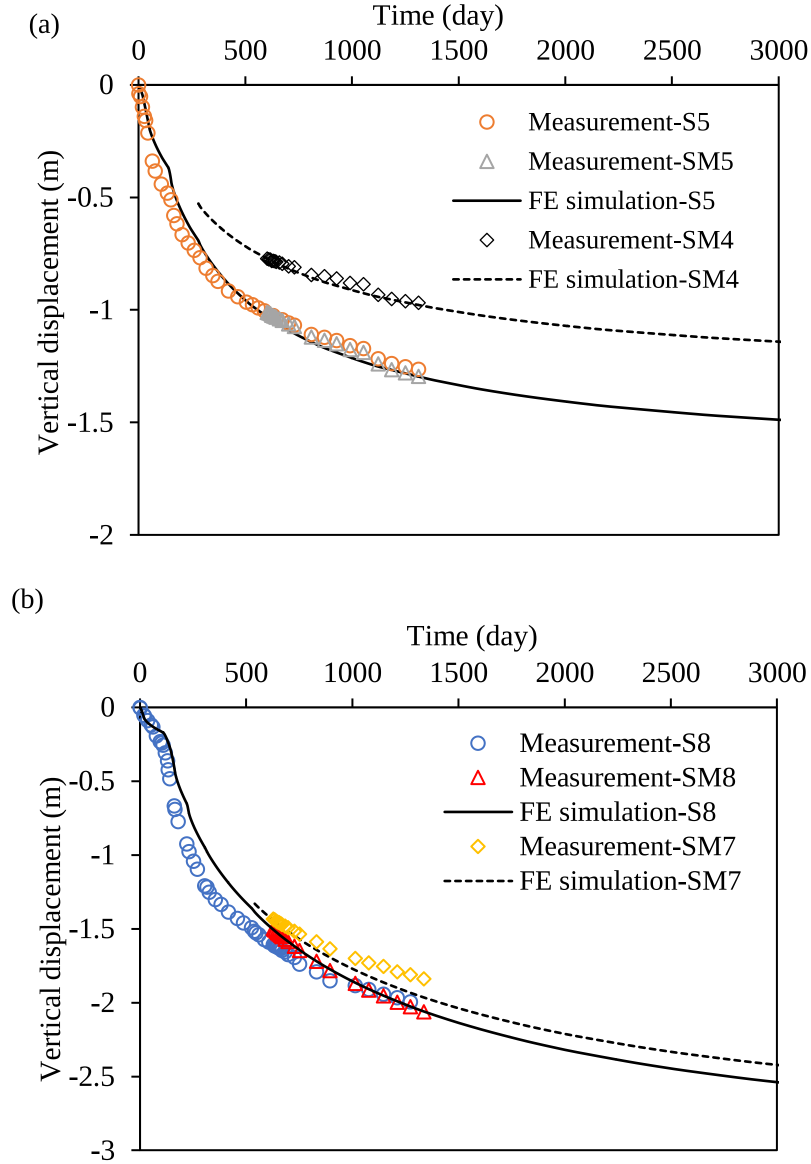

Fig.7. Vertical displacements (settlements) at the different positions of embankments with time by FE simulations and measurement: (a) Scheme 3/2 and (b) Scheme 6/6

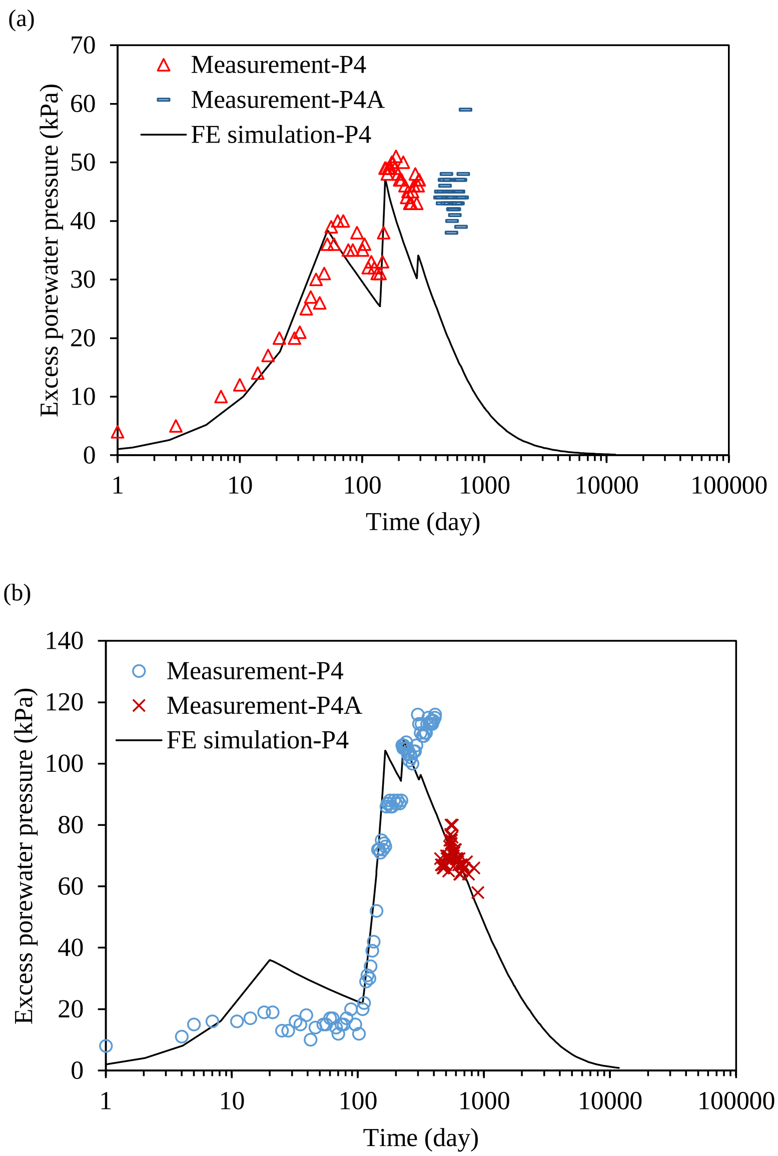

Fig.8. Excess pore water pressures with time by FE simulations and measurement: (a) Scheme 3/2 and (b) Scheme 6/6

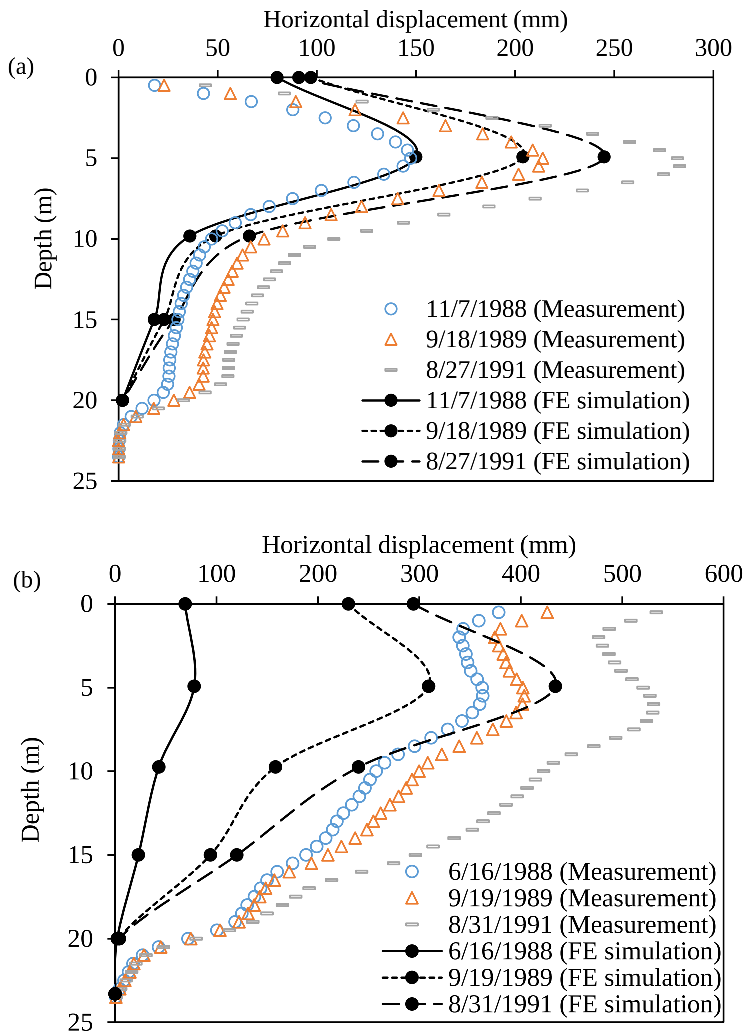

Fig.9. Profiles of horizontal displacements with depth on different dates by FE simulations and measurement: (a) Scheme 3/2 and (b) Scheme 6/6

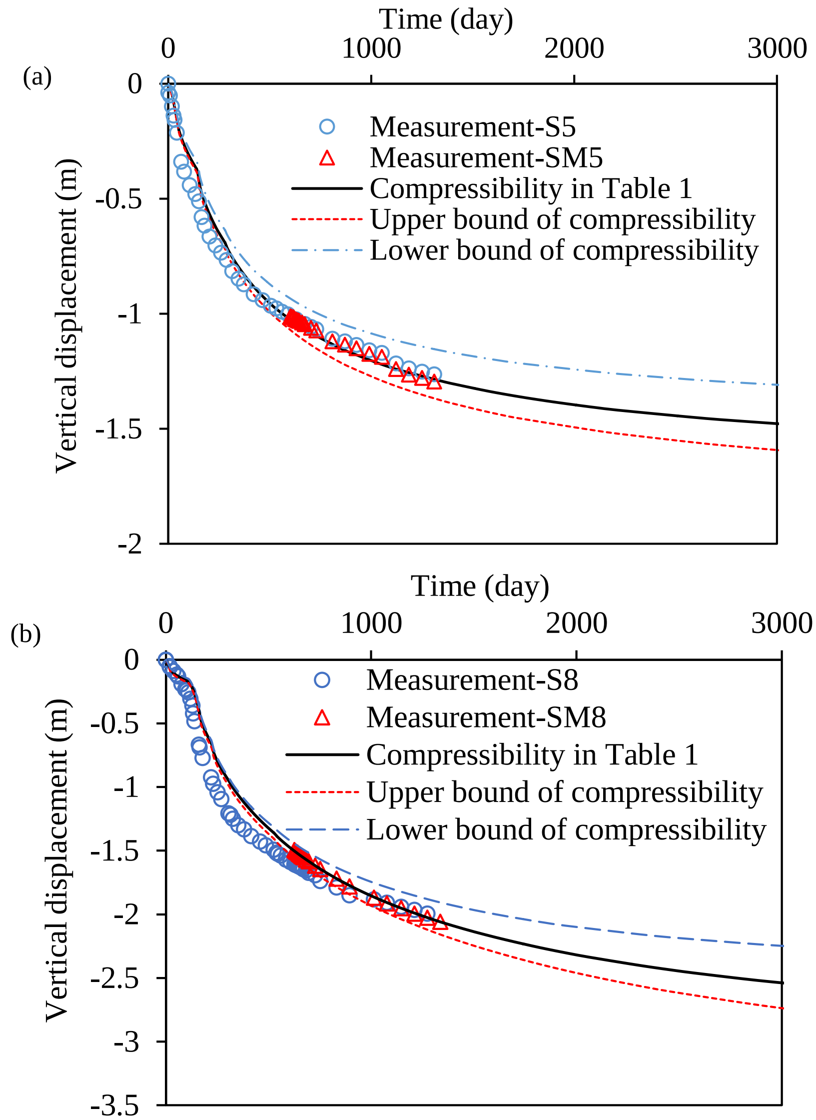

Fig.10. Effects of compressibility parameters on the settlement calculations: (a) Scheme 3/2 and (b) Scheme 6/6

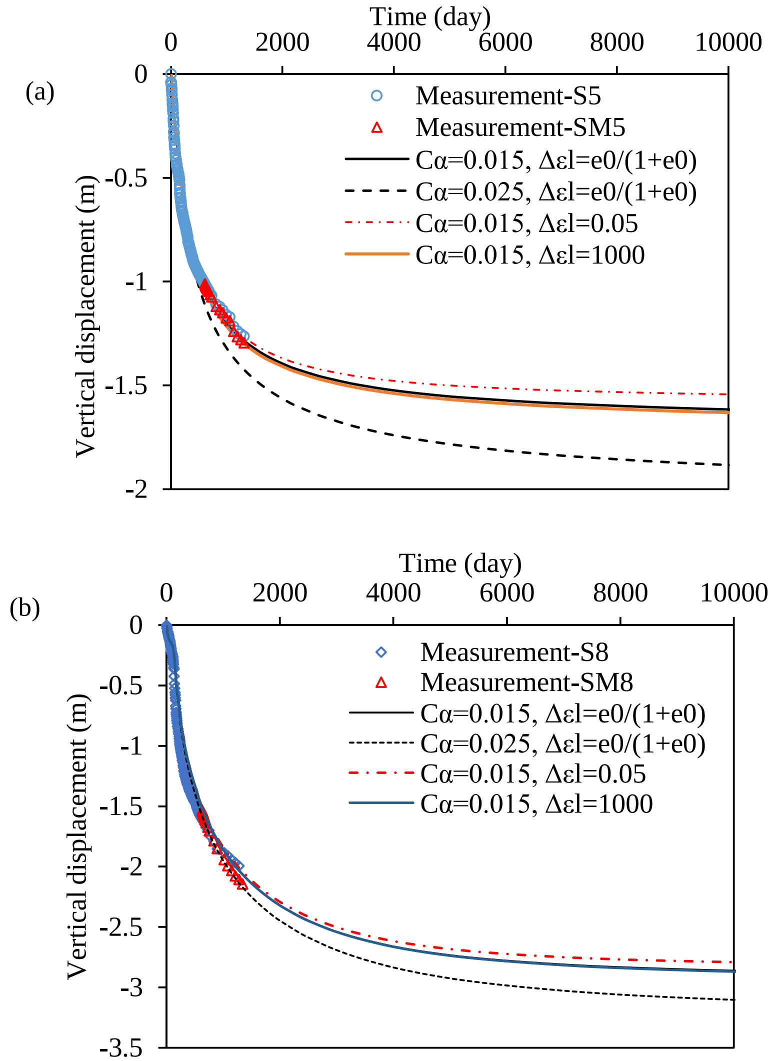

Fig.11. Effects of creep parameters on the settlement calculations: (a) Scheme 3/2 and (b) Scheme 6/6

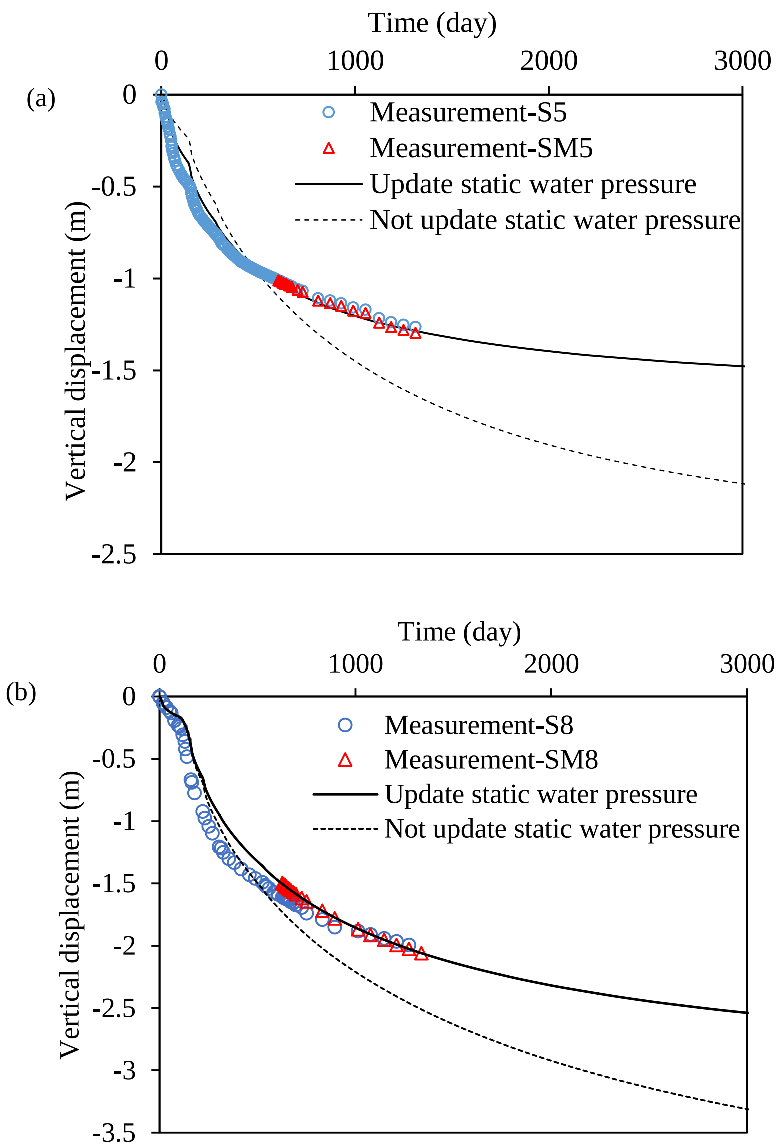

Fig.12. Effects of updating static water pressure on the settlement calculations: (a) Scheme 3/2 and (b) Scheme 6/6

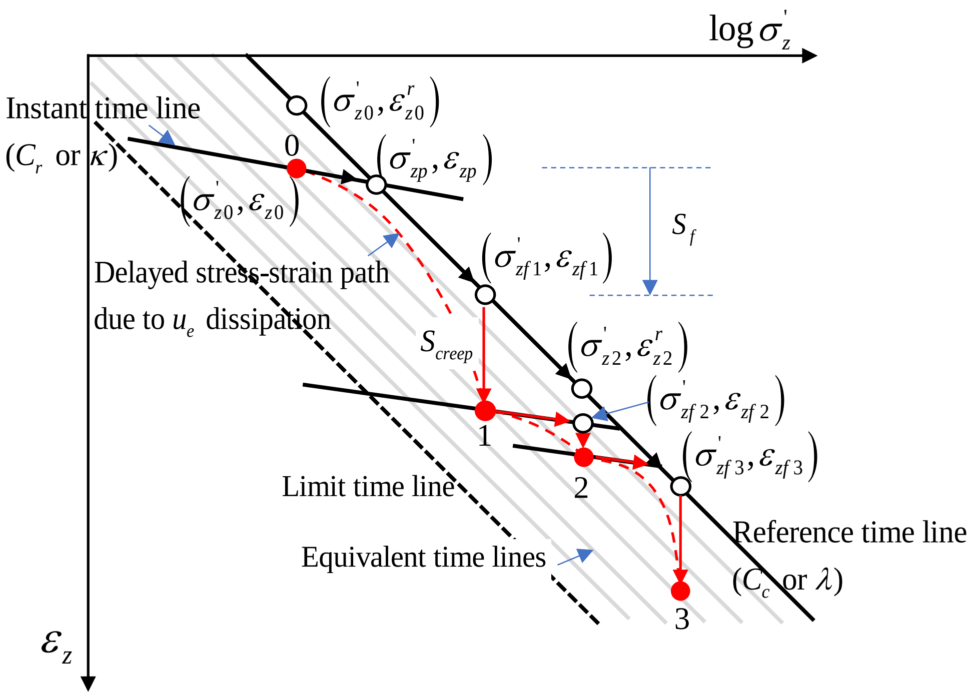

Fig.13. Calculation of creep compression in a 1-D simplified Hypothesis B method (SBM) for multi-staged loading (schematic diagram)

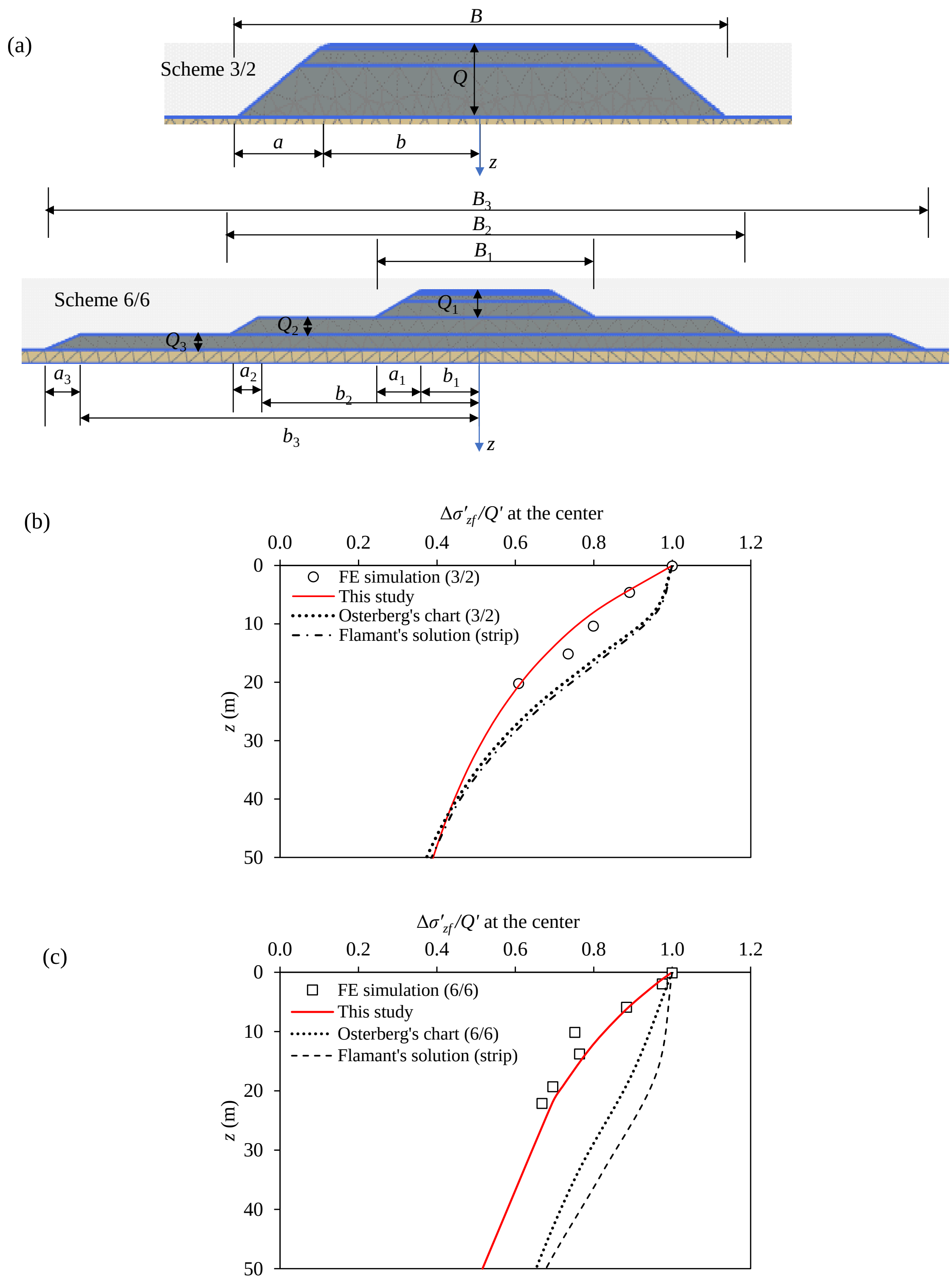

Fig.14. Diffusion of additional stress under embankments: (a) geometry of the embankments, and distribution of normalized total vertical stress with depth for (b) Scheme 3/2 and (c) Scheme 6/6

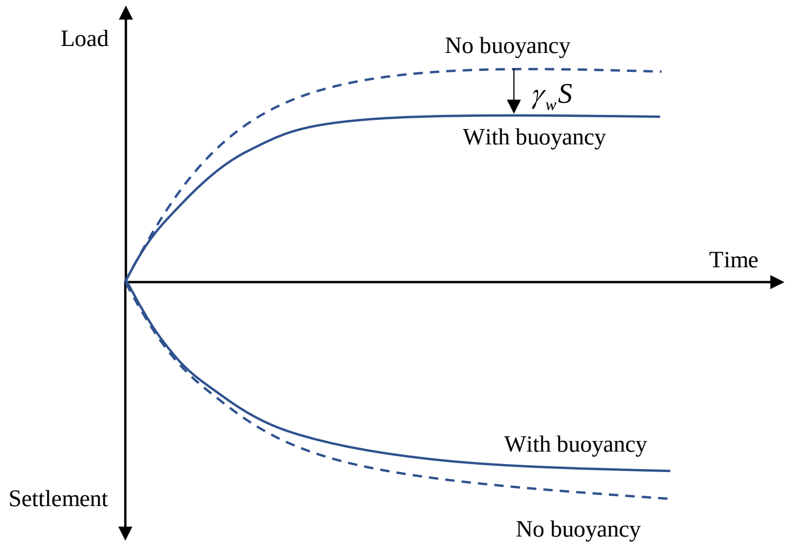

Fig.15. Illustration of buoyancy effect on the embankment loading

(a)

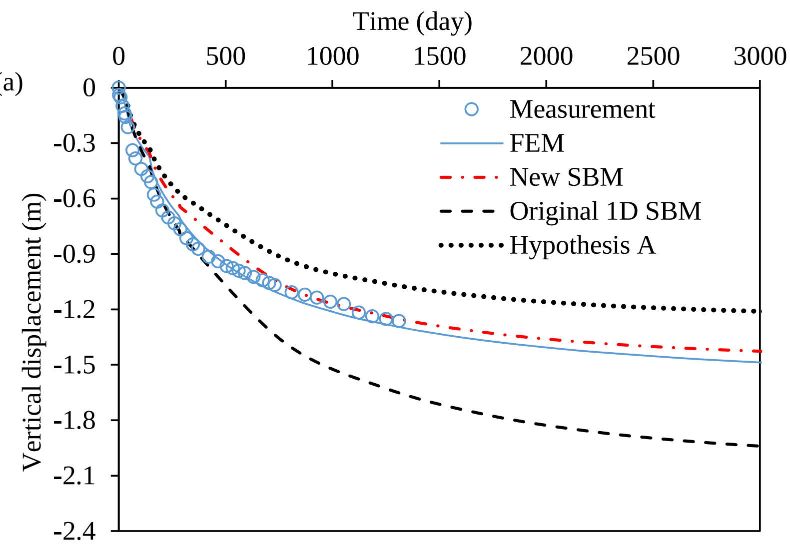

(b)

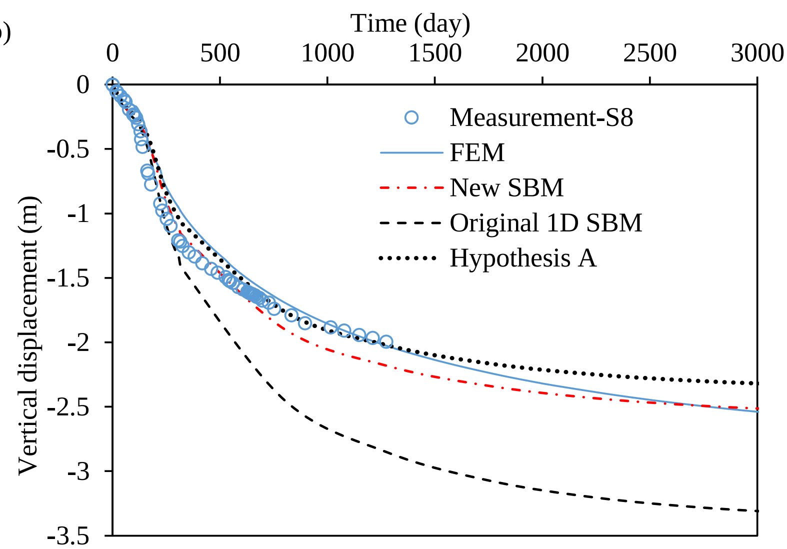

Fig.16. Vertical displacements (settlements) at the center from the simplified Hypothesis B method, FE simulations, and measurement: (a) Scheme 3/2 and (b) Scheme 6/6

Table 1 Soil parameters for Malaysian marine soils

Layer No.	1	2	3	4	5	6	7
Soil type	Crust	Upper clay 1	Upper clay 2	Sandy silty clay	Lower clay	Peat	Sandy clay
Thickness, H (m)	1.8	2.5	2.5	1.6	9.2	0.6	4
Density, γ (kN/m)	16	14.5	14.5	15.5	16	16	16
Initial void ratio, e_0	1.9	3.0	2.5	1.6	1.62	0.54	0.54
POP (kPa)	100	30	16	20	20	90	90
OCR (kPa)	12	2.27	1.46	1.45	1.26	1.84	1.75
Swelling index, κ $\kappa = C_r / \ln(10)$	0.0378	0.087	0.0761	0.0283	0.0342	0.0201	0.0067
Compression index, λ $\lambda = C_c / \ln(10)$	0.378	0.87	0.761	0.283	0.342	0.201	0.067
Creep coefficient, ψ_0 $\psi_0 = C_\alpha / \ln(10)$	0.0065	0.0065	0.0065	0.00587	0.00587	0.00587	0.000826
Creep strain limit, $\Delta\varepsilon_l$ $\Delta\varepsilon_l = e_0 / (1+e_0)$	0.655	0.75	0.714	0.615	0.618	0.351	0.351
Vertical Permeability, k_v (m/s)	2.7×10^{-8}	2.7×10^{-8}	4×10^{-9}	2×10^{-7}	1×10^{-9}	1×10^{-9}	2×10^{-7}
Horizontal permeability, k_h (m/s)	4×10^{-8}	4×10^{-8}	4×10^{-9}	2×10^{-7}	1×10^{-9}	1×10^{-9}	2×10^{-7}
Permeability index, C_k	0.95	0.5	1.25	0.8	0.81	0.27	0.27
Poisson's ratio, ν	0.15	0.15	0.15	0.15	0.15	0.15	0.15
Slope of critical state line, M	1.09	1.07	1.07	1.07	1.07	1.07	1.07